Reactivity of tungsten(v) mononuclear complexes towards Li(TCNQ) and TCNQ. Comparison of the crystal structures of [W(S₂CNMe₂)₄]-[TCNQ] and [Mo(S₂CNMe₂)₄][TCNQ]·MeCN (TCNQ = 7,7,8,8-tetracyanoquinodimethane)‡

Sylvie Le Stang,[a] Françoise Conan,[a] Jean Sala Pala,*,†,[a] Yves Le Mest,[a] Maria-Teresa Garland,[b] Ricardo Baggio,[b] Eric Faulques,[c] Annie Leblanc,[c] Philippe Molinié[c] and Loïc Toupet[d]

[a] Laboratoire de Chimie, Electrochimie Moléculaires et Chimie Analytique, UMR CNRS 6521, Université de Bretagne Occidentale, 6 avenue Le Gorgeu, BP 809, F-29285 Brest Cedex, France
[b] Departamento de Fisica, Facultad de Ciencias Fisicas y Matematicas, Universidad de Chile, Blanco Encalada 2008, Casilla 487-3, Santiago, Chile
[c] Institut des Matériaux, 2 rue de la Houssinière, BP 32229, F-44322 Nantes Cedex 03, France
[d] Groupe Matière Condensée et Matériaux, UMR CNRS 6626, Université de Rennes I, F-35042 Rennes Cédex, France

The reaction of tungsten(v) complexes [W(S₂CNR₂)₄]I (R = Me or Et) with Li(TCNQ) in a dimethylformamide–water mixture at room temperature afforded the new derivatives [W(S₂CNR₂)₄][TCNQ] **1a** and **1b** (TCNQ = 7,7,8,8-tetracyanoquinodimethane). These compounds reacted further with TCNQ in acetonitrile to produce [W(S₂CNR₂)₄][TCNQ]₂ in which the TCNQ moieties are in a mixed-valence state. The physical properties of these new derivatives in solution and in the solid state are presented. The structures of **1a** and of its molybdenum analogue [Mo(S₂CNR₂)₄][TCNQ]·MeCN **2a** have been studied by X-ray diffraction analyses: in **1a** the TCNQ moieties form alternating stacks along the *c* axis according to a quite unusual bond–bond overlap; in **2a** the TCNQ·⁻ moieties are dimerized and exhibit the usual slipped conformation.

The polynitrile derivatives TCNE (tetracyanoethylene) and TCNQ (7,7,8,8-tetracyanoquinodimethane) are well known as π acceptors. They display two reduction processes, easily accessible and reversible, that allow the facile interconversion of three oxidation states among which the TCNX·⁻ radical anion.[1,2] The combination of this property with near planarity explains for TCNQ its propensity to undergo π–π stacking leading to the formation of simple $[(TCNQ)_n]^{n-}$ or complex $[(TCNQ)_n]^{m-}$ anions with *m* < *n* in the solid state. The association of such anions with inorganic cations may lead to mixed organic–inorganic salts possessing interesting features as regards for example their conductive, magnetic and optical properties.[3] In these compounds the inorganic part plays an important role in determining the arrangement of the TCNQ moieties, and often in governing a partial transfer of charge to the TCNQ.[4]

In previous papers we described the chemistry of some molybdenum complexes with the dithiocarbamate ligands S₂CNR₂ towards TCNQ and the syntheses of simple and complex salts were reported.[5] We present here the chemistry of some tungsten analogues and a comparison between the crystal structures of [W(S₂CNMe₂)₄][TCNQ] **1a** and [Mo(S₂CNMe₂)₄][TCNQ]·MeCN **2a**.

Experimental

All reactions were performed in Schlenk tubes in a dry dioxygen-free nitrogen atmosphere. Solvents were distilled by standard techniques and thoroughly deoxygenated before use. Elemental analyses were performed by the Service Central d'Analyses du CNRS, Vernaison, France. Infrared spectra were obtained with a Perkin-Elmer 1430 spectrometer (KBr pellets), Raman spectra with a Fourier-transform spectrometer (Bruker RFS100) at ambient temperature using a ×50 microscope objective and the 1064 nm excitation line of an Nd:YAG laser, ESR spectra either on a JEOL FE 3X (X-band) or a Bruker ER 200D-SRC spectrometer and UV/VIS spectra on an 'Anthélie' (Secoman) spectrometer. The apparatus, the three-compartment micro-electrochemical cell, treatment of solvent and supporting electrolyte for the electrochemical studies have all been previously described.[5a] The reference electrode used was the half-cell: platinum/ferrocenium picrate (10⁻² M), ferrocene (10⁻² M), NBu₄PF₆ (0.2 M), benzonitrile. To compare the present results with those from other works, the ferrocenium–ferrocene formal potential was measured *vs.* the saturated calomel electrode (SCE) in benzonitrile (0.2 M NBu₄PF₆) as +0.43 V. The solid-state magnetic susceptibility measurements were made on powder samples using a commercial SQUID magnetometer from Quantum Design, from 5 to 310 K. Susceptibilities were corrected for the intrinsic diamagnetism of the sample container. Corrections for Pascal diamagnetism, which involve two terms, the first associated with the atomic contributions and the second with structural features such as double or triple carbon–carbon bonds, were not made because the estimation of the second contribution was not precise enough. The starting materials *i.e.* [W(S₂CNR₂)₄]I (R = Me **4a** or Et **4b**) and Li(TCNQ) were prepared as described in the literature.[6,7] The syntheses of the molybdenum derivatives [Mo(S₂CNR₂)₄]-[TCNQ] and [Mo(S₂CNR₂)₄][TCNQ]₂ have been previously described.[5] The TCNQ was from Aldrich.

Preparations

[W(S₂CNMe₂)₄][TCNQ] 1a. An aqueous solution (20 cm³) of Li(TCNQ) (211 mg, 1 mmol) was slowly added at room temperature to a solution of complex **4a** (791 mg, 1 mmol) in dimethylformamide (70 cm³). A slight increase in temperature

was observed; the mixture quickly changed from purple to green. Then, water (50 cm³) was added and a green product was precipitated. It was filtered off, washed with diethyl ether and dried under vacuum. Its recrystallization from acetonitrile (60 cm³) at −20 °C provided dark green rectangular monocrystals in good yield (75%) (Found: C, 32.8; H, 3.3; N, 13.4; W, 20.5. Calc. for $C_{24}H_{28}N_8S_8W$: C, 33.2; H, 3.2, N, 12.9; W, 21.2%). IR (KBr pellets, $\tilde{v}_{max}$/cm⁻¹): 2920w and 2850w (v_{CH}); 2170s and 2150s (v_{CN}); 1545vs (v_{CN}); 835m (δ_{CH}); 355w (v_{WS}). Raman ($\tilde{v}$/cm⁻¹): 195w, 344w, 842m, 1384s, 1609s, 1904w, 2130m, 2182w and 2312w. UV/VIS (MeCN): λ_{max}/nm (log ε) 407 (4.66), 680 (4.05), 743 (4.52), 760 (4.45) and 841 (4.80).

[W(S₂CNEt₂)₄][TCNQ] 1b. A blue aqueous solution (*ca.* 100 cm³) of Li(TCNQ) (180 mg, 0.84 mmol) was added at room temperature to an acetone solution (70 cm³) of complex **4b** (760 mg, 0.84 mmol). A green precipitate immediately appeared. It was filtered off, washed with water and dried under vacuum. Its recrystallization from acetonitrile produced dark green microcrystals (yield 85%) (Found: C, 39.4; H, 4.4; N, 11.4; W, 18.4. Calc. for $C_{32}H_{44}N_8S_8W$: C, 39.2; H, 4.5; N, 11.4; W, 18.8%). IR (KBr pellets, $\tilde{v}_{max}$/cm⁻¹): 2980m, 2940m and 2880w (v_{CH}); 2180s and 2150s (v_{CN}); 1520vs (v_{CN}); 1150s (v_{CS}); 830m (δ_{CH}); 355w (v_{WS}). Raman ($\tilde{v}$/cm⁻¹): 336m, 612w, 977w, 1055vw, 1197m, 1390s, 1532vw, 1600–1613vs, 2162w and 2194m. UV/VIS (MeCN): λ_{max}/nm (log ε) 408 (4.76), 682 (4.13), 745 (4.59), 762 (4.52) and 842 (4.86).

[W(S₂CNMe₂)₄][TCNQ]₂ 5a. An acetonitrile solution (30 cm³) of TCNQ (120 mg, 0.6 mmol) was slowly added at room temperature to a solution of complex **1a** (520 mg, 0.6 mmol) in MeCN (100 cm³). The green mixture was stirred at room temperature for 4 h and filtered. The filtrate was then reduced under vacuum to half its volume and kept for several hours at −20 °C. Fine green microcrystals were isolated after washing with ether (yield 50%) (Found: C, 40.0; H, 2.8; N, 15.2. Calc. for $C_{36}H_{32}N_{12}S_8W$: C, 40.3; H, 3.0; N, 15.7%). IR (KBr pellets, $\tilde{v}_{max}$/cm⁻¹): 2200–2100s (vbr) (v_{CN}); 1550s (v_{CN}); 850–830w (δ_{CH}); 355w (v_{WS}). Raman ($\tilde{v}$/cm⁻¹): 333w, 422m, 613w, 812w, 888w, 1196m, 1383s, 1600–1610s, 1676w and 2102w. UV/VIS (MeCN): λ_{max}/nm (log ε) 393 (5.03), 742 (4.52) and 840 (4.72).

[W(S₂CNEt₂)₄][TCNQ]₂ 5b. The compound TCNQ (50 mg, 0.25 mmol) was added to an acetonitrile solution (50 cm³) of **1b** (220 mg, 0.25 mmol). The green mixture was stirred at room temperature for 3 h. After 2 h at −20 °C fine green needles were isolated and washed with ether (yield 70%) (Found: C, 44.7; H, 4.1; N, 14.3. Calc. for $C_{44}H_{48}N_{12}S_8W$: C, 44.6; H, 4.1; N, 14.2%). IR (KBr pellets, $\tilde{v}_{max}$/cm⁻¹): 2200–2100s, (vbr) (v_{CN}); 1520s (v_{CN}); 850–830w (δ_{CH}); 355vw (v_{WS}). Raman ($\tilde{v}$/cm⁻¹): 335m, 613w, 795w, 1195s, 1387s, 1415w, 1610vs, 1869w, 1940w and 2190w. UV/VIS (MeCN): λ_{max}/nm (log ε) 398 (4.75), 685 (3.72), 747 (4.17), 764 (4.11) and 845 (4.45).

X-Ray crystallography

The powder X-ray studies were carried out using an INEL X-ray diffractometer equipped with a CPS 120 curved detector allowing the recording of powder patterns up to 2θ = 120° (Cu-Kα₁ radiation, λ = 1.540 598 Å).

Crystal parameters and details of the X-ray crystallographic data collection and refinement for compounds **1a** and **2a** are summarized in Table 1. In both cases the unit-cell parameters were determined by least-squares refinement of 25 reflections; intensity data were collected by the ω–2θ scan technique (ambient temperature, up to 2θ = 50°) and corrected for Lorentz-polarization effects. A semiempirical absorption correction (ψ scan) was also applied to **1a**.

Both structures were solved by combining direct methods with Fourier-difference syntheses. Hydrogen atoms were placed
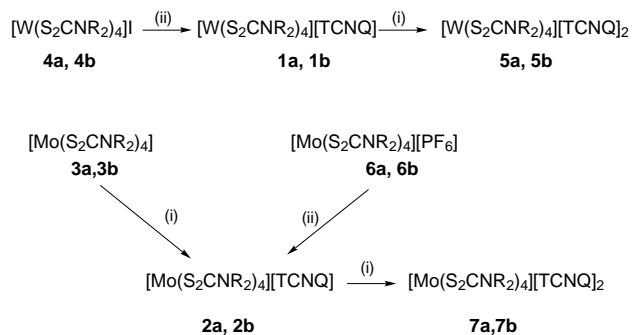
**Scheme 1**   (i) TCNQ, (ii) Li(TNCQ). R = Me **a** or Et **b**

in their ideal positions [d(C–H) = 0.96 Å] and allowed to ride on their corresponding carbon atoms, with isotropic displacement parameters. Both structures were refined by applying full-matrix least squares on F^2. For **1a**, anisotropic thermal parameters were used for all non-hydrogen atoms; the computer programs used were SHELXL 93, SHELXLTL PC and PARST.[8] For **2a**, for which the number of usable independent reflections was low, refinement was done using anisotropic thermal parameters for atoms Mo, S(1) to S(8), C(1), C(4), C(7), C(10) and C(13) to C(19), isotropic parameters for other non-hydrogen atoms and x, y, z fixed for H atoms in order to have a reasonable data/parameters ratio; all the calculations were performed on a Digital Micro VAX 3100 computer with the MOLEN package.[9] In both cases atomic scattering factors were taken from ref. 10.
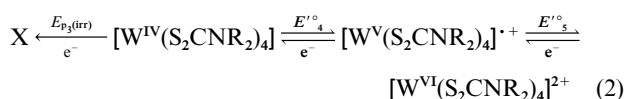
CCDC reference number 186/795.

Results and Discussion

It has been previously shown that the simplest way to obtain the molybdenum(v) compounds [Mo(S₂CNR₂)₄][TCNQ] (R = Me **2a** or Et **2b**) was the oxidation of the molybdenum(iv) derivatives [Mo(S₂CNR₂)₄] **3** by TCNQ (Scheme 1).[5] In order to obtain the tungsten(v) analogues and due to the high sensitivity to dioxygen of the [W(S₂CNR₂)₄] complexes, both in solution and in the solid state,[11] we chose, by comparison with previous works,[7] directly to oxidize the iodide anion by TCNQ in the two tungsten(v) complexes [W(S₂CNR₂)₄]I (R = Me **4a** or Et **4b**). Since no oxidation was observed, the metatheses of **4** with Li(TCNQ) were performed at room temperature; these afforded, after recrystallization in acetonitrile, the new derivatives [W(S₂CNR₂)₄][TCNQ] **1** in the form of green monocrystals for **1a** (R = Me), and dark green microcrystals for **1b** (R = Et) (Scheme 1). Further addition of 1 equivalent of TCNQ to these complexes performed at room temperature in acetonitrile gave the derivatives **5** (R = Me **a** or Et **b**) the elemental analyses of which were in good agreement with a 1:2 stoichiometry [W(S₂CNR₂)₄][TCNQ]₂. The ability of the tungsten compounds **1** to produce complex TCNQ salts is similar to that of their molybdenum analogues.[5]

The cyclic voltammetry (CV) of complexes **1** in benzonitrile solution reveals five redox processes (Fig. 1) of which, by comparison with the TCNQ voltammogram,[12] two reversible systems, one cathodic and one anodic, were assigned to the radical anion TCNQ·⁻, according to equation (1) (Table 2). As

$$TCNQ^{2-} \underset{e^-}{\overset{E'^\circ_1}{\rightleftharpoons}} TCNQ^{\cdot-} \underset{e^-}{\overset{E'^\circ_2}{\rightleftharpoons}} TCNQ \qquad (1)$$
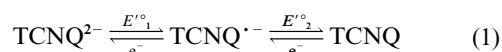
previously described by Nieuwpoort,[6] the three other waves associated with two reversible and one irreversible system can be ascribed to the [W(S₂CNR₂)₄]·⁺ radical cation [equation (2)].

$$X \underset{e^-}{\overset{E_{P_3(irr)}}{\longleftarrow}} [W^{IV}(S_2CNR_2)_4] \underset{e^-}{\overset{E'^\circ_4}{\rightleftharpoons}} [W^V(S_2CNR_2)_4]^{\cdot+} \underset{e^-}{\overset{E'^\circ_5}{\rightleftharpoons}}$$
$$[W^{VI}(S_2CNR_2)_4]^{2+} \qquad (2)$$

Table 1 Crystallographic and refinement data for complexes **1a** and **2a**[a]

	1a	**2a**
Formula	$C_{24}H_{28}N_8S_8W$	$C_{24}H_{28}MoN_8S_8 \cdot CH_3CN$
M	868.87	822.05
Space group	Cc	$P2_1/c$
Crystal size/mm	$0.32 \times 0.18 \times 0.10$	$0.04 \times 0.12 \times 0.32$
Crystal colour, habit	Deep blue, prisms	Deep green, plates
a/Å	12.894(2)	9.254(3)
b/Å	18.666(2)	20.534(4)
c/Å	14.059(2)	19.063(3)
β/°	91.11(1)	90.20(2)
U/Å^3	3383(1)	3623(2)
D_c/Mg m^{-3}	1.71	1.51
$F(000)$	1720	1680
μ(Mo-Kα)/mm^{-1}	3.94	0.828
Diffractometer	Siemens R3m	CAD4 Enraf-Nonius
hkl Ranges	0–15, 0–22, ±16	0–11, 0–24, ±22
Number of reflections collected	3352	6750
Number of independent reflections	3150	6550
R_{int}	0.018	0.029
Observed reflections [$I > n\sigma(I)$]	2802 ($n = 2$)	2346 ($n = 1.2$)
No. refined parameters	370	292
Goodness of fit	1.044	1.39
R, wR	0.021, 0.043[b]	0.095, 0.085[c]
Largest difference peak, hole/e Å^{-3}	0.31, −0.38	0.86, −0.40

[a] Details in common: monoclinic; $Z = 4$; graphite-monochromated Mo-Kα radiation (λ 0.710 73 Å); $R = \Sigma(|F_o| - |F_c|)^2/\Sigma F_o^2$; $wR = [\Sigma w(F_o^2 - F_c^2)^2/\Sigma w(F_o^2)^2]^{\frac{1}{2}}$. [b] $w = [\sigma^2(F_o^2) + (0.0222P)^2]^{-1}$ where $P = (F_o^2 + 2F_c^2)/3$. [c] $w = 1/\sigma(F_o)^2 = [\sigma^2(I) + (0.04F_o^2)^2]^{-\frac{1}{2}}$.

Table 2 Electrochemical data* for complexes **1**, **4** and **5**

Complex	E'°_1	E'°_2	$E_{p,(irr)}$	E'°_4	E'°_5
1a [W(S$_2$CNMe$_2$)$_4$][TCNQ]	−0.84 (60)	−0.23 (60)	−1.92	−1.16 (60)	0.32 (60)
1b [W(S$_2$CNEt$_2$)$_4$][TCNQ]	−0.83 (100)	−0.23 (80)	−2.08	−1.18 (80)	0.34 (100)
5a [W(S$_2$CNMe$_2$)$_4$][TCNQ]$_2$	−0.83 (60)	−0.23 (60)	−1.94	−1.15 (60)	0.32 (60)
5b [W(S$_2$CNEt$_2$)$_4$][TCNQ]$_2$	−0.84 (60)	−0.23 (60)	−2.03	−1.18 (60)	0.32 (60)
4a [W(S$_2$CNMe$_2$)$_4$]I			−1.88	−1.15 (60)	0.31 (60)
4b [W(S$_2$CNEt$_2$)$_4$]I			−2.06	−1.18 (60)	0.32 (60)

* E'° and E_p in V, estimated from CV of solutions of the complexes *ca.* 10^{-3} M in PhCN, 0.2 M NBu$_4$PF$_6$, platinum electrode, scan rate 0.1 V s^{-1}, V *vs.* ferrocenium–ferrocene. Values given in parentheses $\Delta E_p = E_{pa} - E_{pc}$ in mV.

Table 3 Magnetic and ESR data for complexes **1** and **5**

Complex	C/cm^3 K mol^{-1}	θ/K	μ/μ_B	g^a	ΔHpp^{a,b}	g_{inorg}^c (A_w^b)	g_{org}^c
1a	0.32	−3.5	1.60	1.929	40	1.893	2.003
1b	0.70	−0.8	2.37	1.934	57	1.892	2.001
5a	0.38	−7.5	1.74	1.938	48	1.890 (61.5)	2.002
5b	0.47	−1.5	1.94	1.925	68	1.894 (59.3)	2.004

[a] Powder ESR spectra. [b] In 10^{-4} T. [c] Spectra in MeCN.

The CV of compounds **5** has features similar to that of **1** and exhibits the five systems described above, but the peak intensity ratios i_p(TCNQ)/i_p(cation) are twice as high as those of complexes **1**. Moreover, the rotating-disc electrode voltammogram (Fig. 1) clearly shows that the zero current corresponds to half of the TCNQ–TCNQ$^{\cdot-}$ wave.

As previously shown, the charge on the TCNQ moieties in solution may be deduced from UV/VIS spectral examination.[13] Ratios TCNQ:TCNQ$^{\cdot-}$ of *ca.* 0.2:1 for compounds **1a** and **1b** and 1.0 and 1.2:1 respectively for **5a** and **5b** were found.

The ESR spectra of dilute solutions of complexes **1** and **5** (Table 3) are quite similar; they all evidence the existence of two radicals by exhibiting one signal at *ca.* g 2.003 associated with the TCNQ$^{\cdot-}$ entity[14] and a second peak, centred around 1.892. The latter, accompanied by a two-line satellite signal ($A_w = 60 \times 10^{-4}$ T) arising from hyperfine interaction with the ^{183}W nucleus (natural abundance 14.4%, $I = \frac{1}{2}$), is attributed to the [W(S$_2$CNR$_2$)$_4$]$^{\cdot+}$ inorganic cation according to previous work.[6]

All these observations clearly indicate that the dissociation of salts **1** in solution only gives the tungsten(V) radical cation and the TCNQ$^{\cdot-}$ radical anion, while the dissociation of salts **5** produces the same inorganic radical and a TCNQ$^{\cdot-}$–TCNQ mixture in a *ca.* 1:1 ratio; similar observations have been previously reported for the molybdenum analogues.[5]

Crystal structures

The powder X-ray diffraction traces of complexes **1a** and **1b** were run to compare their crystal structures with those of the molybdenum analogues.§ Compound **1b** exhibits a pattern similar to that of its analogue [Mo(S$_2$CNEt$_2$)$_4$][TCNQ] **2b** for which it has been previously shown that the TCNQ$^{\cdot-}$ moieties exist as independent monomers in the solid state.[5] In contrast, for **1a** the 2θ values and the peak intensities clearly reveal the structural differences between this derivative and its molybdenum analogue **2a**; therefore, X-ray analyses were carried out for these two complexes.

The two compounds **1a** and **2a** crystallize in monoclinic

§ A table of 2θ values and peak intensities has been deposited.
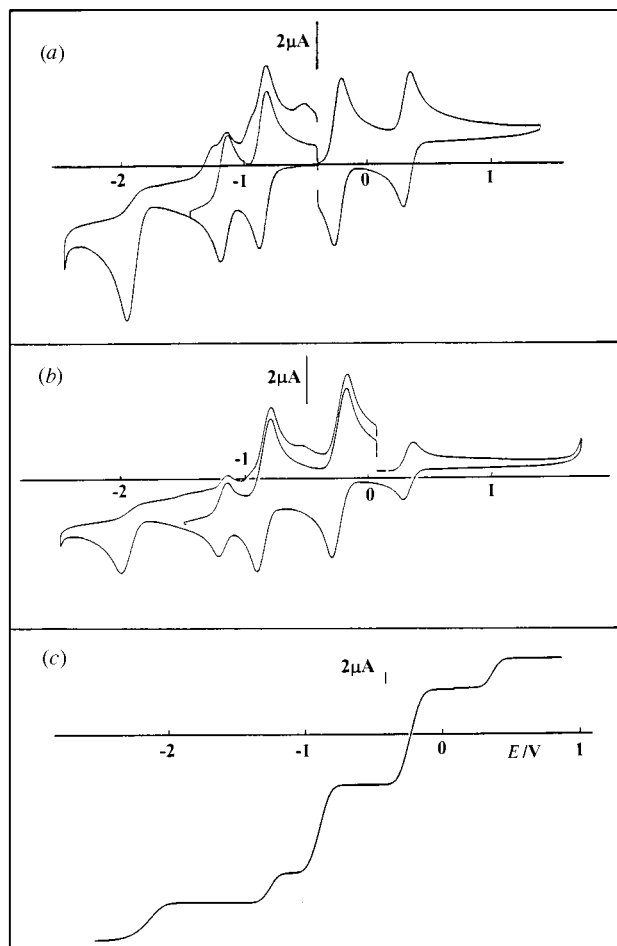
Fig. 1 (*a*) Cyclic voltammogram of complex **1a**, (*b*) cyclic voltammogram of **5a** and (*c*) rotating-disc electrode voltammetry (RDEV) of **5a** (*ca.* 10^{-3} M in PhCN, 0.2 M NBu$_4$PF$_6$, platinum electrode, scan rate 0.1 V s^{-1} for CV, 0.01 V s^{-1} for RDEV, V *vs.* ferrocenium–ferrocene)


Fig. 2 The cation and anion in complex **1a**: atom numbering and TCNQ bond lengths (Å), e.s.d.s in the least significant digits (7), (8) or (9). W–S bond lengths (e.s.d.s in the least significant digits): W–S(1B) 2.491(6), W–S(2B) 2.494(6), W–S(2A) 2.511(6), W–S(1A) 2.532(6), W–S(4B) 2.503(6), W–S(3B) 2.508(6), W–S(4A) 2.542(6), W(1)–S(3A) 2.553(6)

space groups *Cc* and *P*2$_1$/*c*, each unit cell containing four asymmetric units. Both structures consist of four TCNQ anions and four [M(S$_2$CNMe$_2$)$_4$] cations. Four MeCN molecules of solvation are also present in the unit cell of **2a**. The main differences between these two structures concern the TCNQ stacks since both cations are roughly analogous.

In both derivatives there is no crystallographically-imposed symmetry for the TCNQ species. The quinonoid ring is planar within experimental error, the most important departures from the overall mean plane being found for the terminal N atoms [for example 0.19 Å for N(6B) in **1a**]. In **1a** the overall shape and size parameters of the TCNQ species are quite normal, whereas in **2a** rather high estimated standard deviations (e.s.d.s) were found for bond lengths and angles; this precludes a direct comparison of the TCNQ geometries in the two structures (Figs. 2 and 3).

Flandrois and Chasseau[15] have pointed out that the charge on a TCNQ unit can be estimated from the difference between the lengths of the formally single and formally double bonds of the pseudo-quinonoid ring (respectively *b* and *a* in Table 4).[15] The bond lengths observed for **1a** (Fig. 2 and Table 4) are close to those found in Rb(TCNQ)[16] and rather different from those in neutral TCNQ.[17] A charge of -1.25 is calculated from the Kistenmacher relation,[18] close to that observed for the molybdenum derivative [Mo(S$_2$CNEt$_2$)$_4$][TCNQ] **2b**.[5] Significant differences exist in **2a** between *a priori* equivalent carbon–carbon bonds (for instance *b* from 1.38 to 1.44 Å) (Fig. 3) and the charge (-0.92) is only tentatively given.[18]

A careful examination of the literature shows that various TCNQ arrangements may arise in the solid state; the TCNQ moieties can exist as isolated monomers[5,14,19] or lead to regular or complex chains by various stacks. One of the more usual
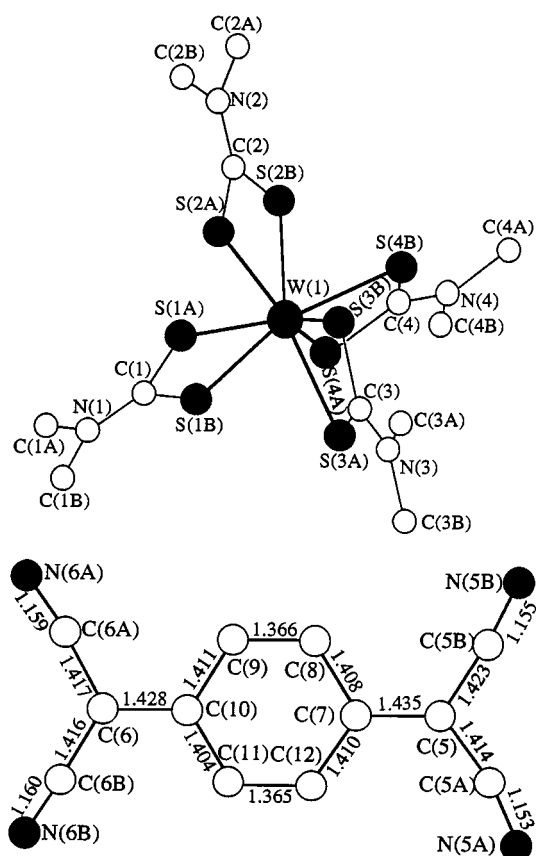
arrangements concerns [(TCNQ)$_2$]$^{2-}$ dimer units. Such dimers often exhibit slipped conformations where slipping takes place either along the short or long TCNQ axis; this enables the so-called (i) ring–ring (R–R),[20] (ii) ring–external bond (R–B)[4,21] and (iii) external bond–external bond (B–B)[4,22] overlaps. However, they may also exist with an almost perfectly eclipsed geometry.[23]

The TCNQ moieties of complex **1a** form alternating stacks along the *c* axis as shown in Fig. 4. Adjacent TCNQ species are crystallographically equivalent and exhibit a quite unusual B–B overlap. The planes of successive units are not exactly parallel and exhibit a 9° dihedral angle and a mean interplanar distance of *ca.* 3.3 Å. Short contacts between successive moieties are observed [C(11)···N(5B) 3.26 Å].

As clearly shown in Fig. 5, in compound **2a** the TCNQ$^{·-}$ units are dimerized according to a usual R–R overlap with a short-axis slipping of *ca.* 0.8 Å. In the centrosymmetric dimeric units the quinonoid rings display interplanar and barycentre distances of 3.15 and 3.29 Å respectively. Such an arrangement is quite similar to that of [{Fe(η-C$_5$Me$_5$)$_2$}$_2$][TCNQ]$_2$ in which the intradimer distance is 3.147 Å.[24]

In both [M(S$_2$CNMe$_2$)$_4$] groups the metal is surrounded by eight sulfur atoms from four almost equivalent S$_2$CNMe$_2$ ligands which are basically planar; they however present various twisting angles around the N–C bond, which range from 1.3° for C(1)–N(1) to 2.9° for C(2)–N(2) in complex **1a** (Figs. 2 and 3). Analysis of the resulting MS$_8$ polyhedron by the Kepert procedure[25] indicates that its geometry at the M site is best described as a D_{2d} dodecahedron. The co-ordination sphere of **1a** can be described as two interpenetrating trapezoids, T$_1$ and T$_2$, respectively defined by S(1A), S(1B), S(4A), S(4B) and S(2A), S(2B), S(3A), S(3B), which intersect at the cation site

Table 4 Comparison of some bond lengths (Å) and estimation of the charge of the TCNQ moiety
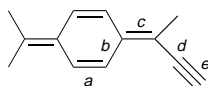
Compound	Ref.	a	b	c	d	e	$b-c$	$c-d$	$c/(b+d)$	$(a+c)/(b+d)$	ρ^a
1a	This work	1.365(7)	1.408(7)	1.431(9)	1.418(9)	1.156(9)	−0.023	0.013	0.506	0.989	−1.25
2a	This work	1.37(2)	1.41(2)	1.405	1.41(2)	1.15(3)	0.005	−0.005	0.498	1.02	b
2b	5	1.356(8)	1.416(8)	1.451(8)	1.404(9)	1.148(9)	0.001	0.011	0.502	0.983	−1.08
Rb(TCNQ)	16	1.373(1)	1.423(3)	1.420(1)	1.416(8)	1.153(7)	0.003	0.004	0.500	0.984	−1
TCNQ	17	1.346(3)	1.448(4)	1.374(3)	1.441(4)	1.140(1)	0.074	−0.067	0.476	0.942	0

^{a} Estimated charge of the TCNQ unit using the Kistenmacher relation [18] $\rho = A[c/(b+d)] + B$ with $A = -41.667$ and $B = 19.833$. ^{b} Found to be −0.92 but only tentatively given since bond length e.s.d. values are large.
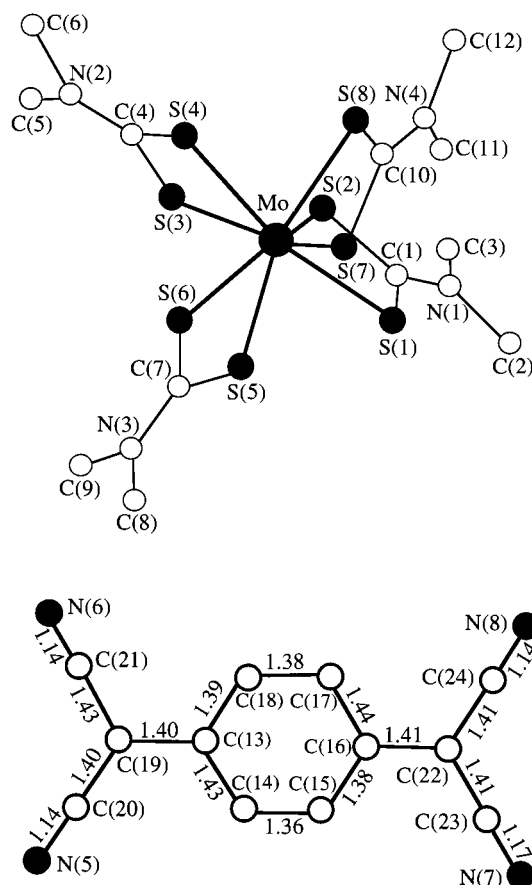
Fig. 3 The cation and anion in complex **2a**: atom numbering and TCNQ bond lengths (Å), e.s.d.s in the least significant digits (2). Mo−S bond lengths (e.s.d.s in the least significant digits): Mo−S(1) 2.492(4), Mo−S(2) 2.523(4), Mo−S(3) 2.468(4), Mo−S(4) 2.549(4), Mo−S(5) 2.528(4), Mo−S(6) 2.491(4), Mo−S(7) 2.526(4), Mo−S(8) 2.489(4)

and are almost perpendicular to each other (dihedral angle 90.3°). These trapezoids, though slightly twisted, do not deviate severely from planarity: their mean, maximum departures are respectively 0.038, 0.058 Å for S(4A) in T_1 and 0.059, 0.091 Å for S(2A) in T_2. The experimental values for φ_A and φ_B, i.e. the angles made by the M−A ('polar' bond) and M−B ('equatorial' bond) bonds respectively with the four-fold inversion axis ($\varphi_A = 35.0$, $\varphi_B = 102.9°$) are lower than expected (39.0 and 106.5° respectively) for a normalized bite [$b =$ (W−S/S−S) = 1.12]. This is a well known fact resulting from the slightly different lengths measured for 'polar' bonds (labelled **A**) and 'equatorial' bonds (labelled **B**).[25] The former (mean 2.534 Å) are slightly larger than the latter (mean 2.499 Å); this is explained by the more important interligand repulsion at the polar sites. The WS$_8$ polyhedron is very similar to those appearing in closely related structures, viz. [W(S$_2$CNEt$_2$)$_4$]Br[26] and [W(S$_2$CSEt)$_4$][27] ($b =$

1.11, 1.12; $\varphi_A = 34.6$, 35.8°; $\varphi_B = 102.4$, 102.8°; $\theta_A - \theta_B = 0.9$, 1.5°). A close inspection of the Kepert parameters suggests that the most noticeable difference between the co-ordination spheres is a slightly larger trapezoid twisting ($\Delta\theta$) in **1a**.

The geometrical features of the MoS$_8$ polyhedron in complex **2a** are quite similar to those reported above [T_1: S(1), S(2), S(3), S(4). T_2: S(5), S(6), S(7), S(8). T_1T_2 dihedral angle 90.4°; polar Mo−S bond lengths ranging from 2.523(4) to 2.549(4) Å, equatorial Mo−S from 2.468(4) to 2.492(4) Å].

Infrared studies

The IR spectra of compounds **1** are quite similar and exhibit the characteristic vibrations of the TCNQ$^{\cdot-}$ radical and the main features of the [W(S$_2$CNR$_2$)$_4$]$^{\cdot+}$ inorganic cation.[6,10] In both cases two sharp and intense bands at 2170, 2150 cm^{-1} for **1a** and at 2180, 2150 cm^{-1} for **1b** are attributable to the ν_{CN} vibrations.[12b,19a] The δ_{CH} frequency values (ca. 830 cm^{-1}) for both complexes corroborate the ionic nature of the TCNQ group[28] and clearly indicate that these compounds are simple TCNQ salts. Furthermore, the missing a$_g$ activated modes ν_{3-9} confirm the monomeric nature of **1b** in the solid state.

The IR spectra of compounds **5** strongly differ from those described above since they display bands attributable to highly delocalized electronic structures,[28] i.e. a broad band at ca. 2220–2100 cm^{-1} assigned to the ν_{CN} vibrations and two bands at 850 and 830 cm^{-1}, characteristic of the δ_{CH} vibrations. The band pattern, similar to the IR spectrum of [Rh(nbd)(bpy)]-[TCNQ]$_2$ {nbd = bicyclo[2.2.1]heptane-2,5-diene (norbornadiene), bipy = 2,2′-bipyridine},[28b] unambiguously indicates the existence of a complex anion resulting from strong electronic interactions between the TCNQ moieties.

Raman studies

Raman spectra of pristine TCNQ single crystals exhibit characteristic lines at 1206s, 1453vs, 1601vs, 2190vw and 2221vs cm^{-1}. These bands are attributable respectively to the following vibrations:[5] ν_5 (a mixing of ring stretch and CH bend), ν_4 (C=C stretch of the ring), ν_3 (a mixing of C=C and C−C stretchings), ν_{42} and ν_2 (CN stretch). For compound **1b** these lines are shifted to 1197m, 1390s, 1600–1613vs, 2162w, and 2194m cm^{-1}; these features vanish in intensity for **1a** for which lines remain at 1384s, 1609s, 2130m and 2182w cm^{-1}. The lines are shifted to 1196m, 1383s, 1600–1610s and 2102w cm^{-1} for **5a**, and to 1195s, 1387s, 1610vs and 2190w cm^{-1} for **5b**.

The most relevant change in the Raman spectra is the strong shift of ν_4 at 1453 cm^{-1} for pristine TCNQ towards 1380–1390 cm^{-1} for these materials. This is the signature of a quasi-complete reduction of TCNQ^0 in TCNQ$^{\cdot-}$ and therefore characterizes the charge transfer of one electron onto the TCNQ ring in the salts.[5] The scattering of the CN bonds is somewhat perturbed since the high-frequency component at 2221 cm^{-1} does not occur and the lowest-frequency component at ca. 2190 cm^{-1} has a relatively strong intensity. This change can be
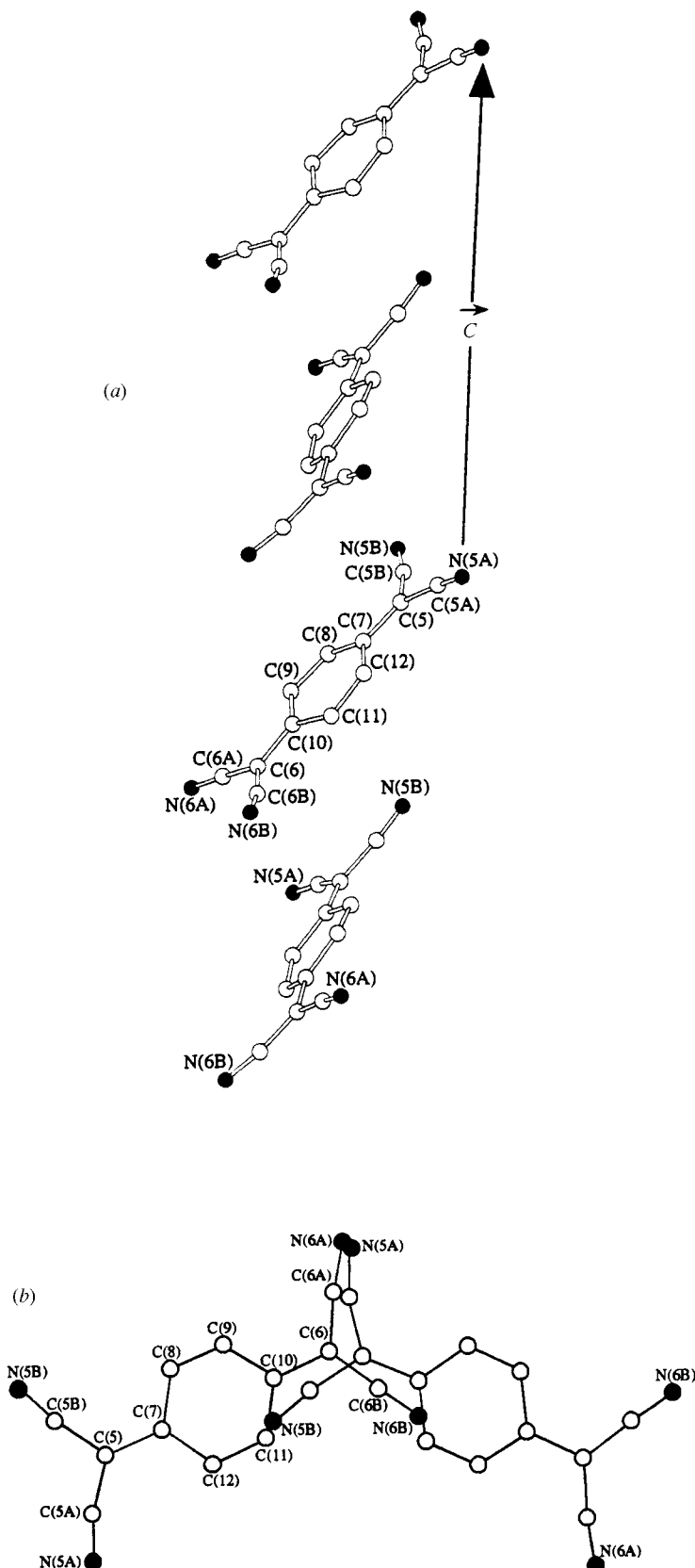
Fig. 4 Views showing (*a*) the TCNQ stack along the *c* axis and (*b*) the overlap between two TCNQ units in complex **1a**

explained by the modification of the Raman selection rules due to the different crystalline environments of the TCNQ moieties in the complexes. On the whole the Raman results agree well with the above-mentioned IR data.

Magnetic studies

Solid-state magnetic susceptibility measurements were per-

formed on compounds **1** and **5** in the 5–310 K temperature range. The $\chi_m T$ *vs.* T curves for compounds **1** are shown in Fig. 6. The magnetic susceptibilities for these four compounds obey a Curie–Weiss law $\chi = C/(T - \theta)$ with characteristics given in Table 3.

For compound **1a** the effective moment value ($\mu_{eff} = 1.60\ \mu_B$) is in good agreement with the existence of a single $S = \frac{1}{2}$ spin. Thus, it seems very likely that the magnetic susceptibility values
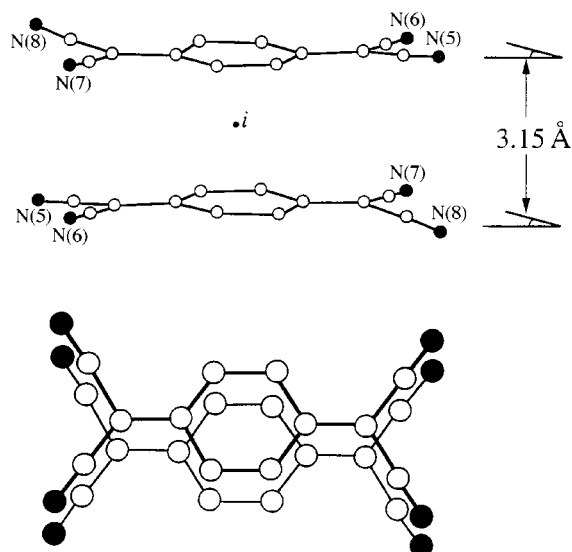
Fig. 5 Two different views of the [(TCNQ)$_2$]$^{2-}$ dimer in complex **2a** showing the overlap and the interplanar distance between the two TCNQ units
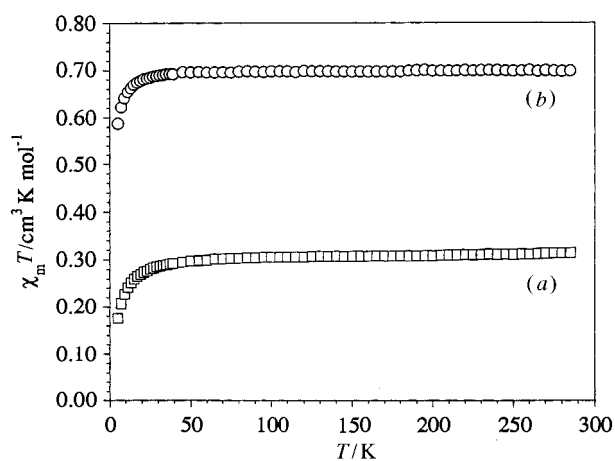

Fig. 6 Plots of $\chi_m T$ *vs. T* within the 5–300 K temperature range: (*a*) complex **1a**, (*b*) **1b**
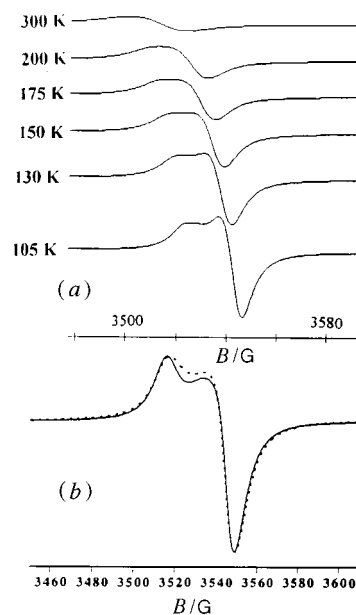

Fig. 7 Powder ESR spectra for complex **1a**: (*a*) evolution within the 105–300 K temperature range, (*b*) experimental and simulated (dotted line) ESR spectra at 105 K, (*c*) temperature dependencies of the *g* factor for **1a** and **2a**

correspond only to the contribution of the radical cation, although X-ray and infrared analyses did not clearly demonstrate the existence of a dimeric [(TCNQ)$_2$]$^{2-}$ anion. The μ_{eff} value (2.37 μ_B) of **1b** is close to the magnetic moment (2.47 μ_B) found for the molybdenum analogue [Mo(S$_2$CNEt$_2$)$_4$][TCNQ] **2b**. The effective moment of two non-interacting spins given by equation (3) is in good agreement with our experimental results,

$$\mu_{eff}^2 = g_{cation}^2[S(S+1)] + g_{anion}^2[S(S+1)] \qquad (3)$$

both values being consistent with the existence of two isolated $S = \frac{1}{2}$ spins, the TCNQ$^{\cdot-}$ radical anion and the [M(S$_2$C-NEt$_2$)$_4$]$^{\cdot+}$ radical cation. Such a behaviour has been previously described for [Fe(C$_{15}$H$_{22}$N$_6$B)$_2$][TCNQ].[29]

Compounds **5** present behaviours comparable with that of **1a** since the μ_{eff} values (1.74 and 1.94 μ_B respectively for **5a** and **5b**) show that the magnetic susceptibilities mainly result from the $S = \frac{1}{2}$ [W(S$_2$CNR$_2$)$_4$]$^{\cdot+}$ system.

The weak θ values for all the studied derivatives suggest the existence of slight antiferromagnetic interactions at very low temperatures which could be assigned to the inorganic cation as a similar behaviour was previously observed for the molybdenum complex [Mo(S$_2$CNMe$_2$)$_4$][PF$_6$].[30]

The room-temperature powder ESR spectra of complexes **1** and **5** are very alike since only one peak at *ca.* 1.93 (ΔH_{pp} from 40 to 68 10^{-4} T) is observed in all of them. The spectra of the

molybdenum analogues are similar and the existence of magnetic interactions between the organic and inorganic anions in each compound is suggested (Table 3).

In order to compare the magnetic behaviour of compounds **1a** and **2a** which strongly differ in their organic stacks, ESR studies were run over a large temperature range (105–360 K for **1a**, 105–300 K for **2a**) (Fig. 7). For **1a** the *g* factor is shifted from 1.901 (105 K) to 1.924 (360 K). The temperature increase results in an obvious evolution of the spectra. While at 105 K the spectrum displays a signal characteristic of axial symmetry ($g_\perp = 1.913$ and $g_\parallel = 1.897$), the two systems collapse to give a broad signal at *ca.* 175 K. Comparison of $g_\perp$ and $g_\parallel$ values with those reported by Nieuwpoort[6] for the [M(S$_2$CNMe$_2$)$_4$]$^+$ cations (M = Mo or W) clearly indicates an inorganic origin for the detected radical at low temperature.[6] For compound **2a**, in the whole temperature range, the spectra display similar features and there is no significant shift of the *g* value.

Discussion

The magnetic properties of complex **1b** are consistent with the crystallographic data; they both indicate the existence of essentially isolated cationic and anionic radicals, although ESR measurements suggest weak interactions. The lack of an organic contribution to the magnetic behaviour of **1a**, **5a** and **5b** suggests strong interactions between the TCNQ species. As previously shown, two TCNQ$^{\cdot-}$ or [(TCNQ)$_2$]$^{\cdot-}$ moieties can interact to form respectively simple [(TCNQ)$_2$]$^{2-}$ or complex [(TCNQ)$_m$]$^{n-}$ anions in the $S = 0$ ground state.[21a,31] Such a hypothesis may be applied for compounds **1a**, **5a** and **5b**.

For the dimethyldithiocarbamatotungsten complex **1a** the

crystallographic studies did not show the existence of isolated dimeric $[(TCNQ)_2]^{2-}$ units; the TCNQ form alternating stacks along the c axis according to a B–B overlap with short TCNQ unit contacts (3.26 Å) which could explain the magnetic behaviour and be associated with conduction properties.[32] In the absence of suitable single crystals, such a hypothesis could not be corroborated by conductivity measurements. In the molybdenum analogue **2a** the TCNQ units form isolated dimers in a slipped R–R conformation. Both complexes display quite similar magnetic properties since only the contribution of the radical cation is observed.

For the isostructural diethyldithiocarbamato complexes **1b** and **2b** the magnetic measurements are consistent with the existence of two isolated $S = \frac{1}{2}$ spins, the radical cation and the $TCNQ^{\bullet-}$ radical anion. These results are consistent with the crystal structure in which the TCNQ units form independent radical monomers.

Acknowledgements

References

1 W. Kaim and M. Moscherosch, *Coord. Chem. Rev.*, 1994, **129**, 157.
2 H. Endres, *Extended Linear Chain Compounds*, ed. J. S. Miller, Plenum, New York, 1983, p. 263.
3 R. P. Shibaeva and L. O. Atovmyan, *J. Struct. Chem. (Engl. Transl.)*, 1972, **13**, 514.
4 A. Bencini and C. Zanchini, *Inorg. Chem.*, 1991, **30**, 4245.
5 (*a*) M. Decoster, F. Conan, J. E. Guerchais, Y. Le Mest, J. Sala Pala, J. C. Jeffery, E. Faulques, A. Leblanc and P. Molinié, *Polyhedron*, 1995, **14**, 1741; (*b*) E. Faulques, A. Leblanc, P. Molinié, M. Decoster, F. Conan, J. E. Guerchais and J. Sala Pala, *Spectrochim. Acta, Part A*, 1995, **51**, 805.
6 A. Nieuwpoort, Ph.D. Thesis, Nijmegen, 1975.
7 L. R. Melby, R. J. Harder, W. R. Hertler, W. Mahler, R. E. Benson and W. E. Mochel, *J. Am. Chem. Soc.*, 1962, **84**, 3374.
8 G. M. Sheldrick, SHELXL 93, Program for Crystal Structure Refinement, University of Göttingen, 1993; SHELXTL PC, Version 4.2, Siemens Analytical X-Ray Instruments, Madison, WI, 1991; M. Nardelli, PARST, *Comput. Chem.*, 1983, **7**, 95.
9 C. K. Fair, MOLEN, An Interactive Intelligent System for Crystal Structure Analysis, Enraf-Nonius, Delft, 1990.
10 *International Tables for X-Ray Crystallography*, Kynoch Press, Birmingham, 1974, vol. 4.
11 D. A. Brown, W. K. Glass, H. J. Toma and W. E. Waghorne, *J. Chem. Soc., Dalton Trans.*, 1987, 2531.
12 (*a*) M. Moscherosch, E. Waldhör, H. Binder, W. Kaim and J. Fiedler, *Inorg. Chem.*, 1995, **34**, 4326; (*b*) S. E. Bell, J. S. Field, R. J. Haines, M. Moscherosch, W. Matheis and W. Kaim, *Inorg. Chem.*, 1992, **31**, 3269; (*c*) S. G. Clarkson, B. C. Lane and F. Basolo, *Inorg. Chem.*, 1972, **11**, 662.
13 H. T. Jonkman and J. Kommandeur, *Chem. Phys. Lett.*, 1972, **15**, 496; P. Baird, J. A. Bandy, M. L. H. Green, A. Hammet,

E. Marseglia, D. S. Obertelli, K. Prout and J. Qin, *J. Chem. Soc., Dalton Trans.*, 1991, 2377; J. Pecherz, M. Kryszewski and A. Tracz, *J. Macromol. Sci., Chem.*, 1991, **28**, 623; W. Pukacki, M. Pawlak, M. Lequan and R. M. Lequan, *Inorg. Chem.*, 1987, **26**, 1328.
14 P. J. Spellane, L. V. Interrante, R. K. Kullnig and F. S. Tham, *Inorg. Chem.*, 1989, **28**, 1587.
15 S. Flandrois and D. Chasseau, *Acta Crystallogr., Sect. B*, 1977, **33**, 2744.
16 A. Hoekstra, T. Spoelder and A. Vos, *Acta Crystallogr., Sect. B*, 1972, **28**, 14.
17 R. E. Long, R. A. Sparks and K. N. Trueblood, *Acta Crystallogr.*, 1965, **18**, 932.
18 T. J. Kistenmacher, T. J. Emge, A. N. Bloch and D. O. Cowan, *Acta Crystallogr., Sect. B*, 1982, **38**, 1193.
19 (*a*) V. J. Murphy and D. O'Hare, *Inorg. Chem.*, 1994, **33**, 1833; (*b*) C. Campana, K. R. Dunbar and X. Ouyang, *Chem. Commun.*, 1996, 2427.
20 M. C. Muñoz, J. Cano, R. Ruiz, F. Lloret and J. Faus, *Acta Crystallogr., Sect. C*, 1995, **51**, 873; P. Lacroix, O. Kahn, A. Gleizes, L. Valade and P. Cassoux, *Nouv. J. Chim.*, 1984, **8**, 643; M. T. Azcondo, L. Ballester, A. Gutierrez, M. F. Perpiñan, U. Amador, C. Ruiz-Valero and C. Bellitto, *J. Chem. Soc., Dalton Trans.*, 1996, 3015; M. C. Grossel, F. A. Evans, J. A. Hrijac, J. R. Morton, Y. Le Page, K. F. Preston, L. H. Sutcliffe and A. J. Williams, *J. Chem. Soc., Chem. Commun.*, 1990, 439.
21 (*a*) S. Z. Goldberg, B. Spivack, G. Stanley, R. Eisenberg, D. M. Braitsch, J. S. Miller and M. Abkowitz, *J. Am. Chem. Soc.*, 1977, **99**, 110; (*b*) I. V. Rozdestvenskaja, I. I. Bannova, G. G. Abashev, V. S. Russkikh and O. A. Usov, *Z. Kristallogr.*, 1996, **211**, 258.
22 H. Oshio, E. Ino, I. Mogi and T. Ito, *Inorg. Chem.*, 1993, **32**, 5697; G. E. Matsubayashi, T. Iinuma, T. Tanaka, K. Oka and K. Nakatsu, *Inorg. Chim. Acta*, 1985, **102**, 145.
23 M. Decoster, F. Conan, Y. Le Mest, J. Sala Pala, A. Leblanc, P. Molinié, E. Faulques and L. Toupet, *New J. Chem.*, 1997, **21**, 215.
24 A. H. Reis, L. D. Preston, J. M. Williams, S. W. Peterson, G. A. Candela, L. J. Swartzendruber and J. S. Miller, *J. Am. Chem. Soc.*, 1979, **101**, 2576.
25 D. L. Kepert, *Prog. Inorg. Chem.*, 1978, **24**, 179.
26 J. G. Wijnhoven, *Cryst. Struct. Commun.*, 1973, **2**, 637.
27 K. Hanewald, G. Kiel and G. Gattow, *Z. Anorg. Allg. Chem.*, 1981, **476**, 89.
28 (*a*) L. Ballester, M. C. Barral, R. Jiménez-Aparicio and B. Olombrada, *Polyhedron*, 1996, **15**, 211; (*b*) L. Ballester, A. Gutierrez, R. Jiménez and M. F. Perpiñan, *Polyhedron*, 1996, **15**, 295; (*c*) L. Ballester, M. C. Barral, A. Gutierrez, A. Monge, M. F. Perpiñan, C. Ruiz-Valero and A. E. Sanchez-Pélaez, *Inorg. Chem.*, 1994, **33**, 2142; (*d*) S. T. Bartley and K. R. Dunbar, *Angew. Chem., Int. Ed. Engl.*, 1991, **30**, 448; (*e*) M. Inoue and M. B. Inoue, *J. Chem. Soc., Faraday Trans. 2*, 1985, 539.
29 S. J. Mason, C. M. Hill, V. J. Murphy, D. O'Hare and D. J. Watkin, *J. Organomet. Chem.*, 1995, **485**, 165.
30 M. Decoster, Ph.D. Thesis, Université de Bretagne Occidentale, 1994.
31 J. R. Morton, K. F. Preston, M. D. Ward and P. J. Fagan, *J. Chem. Phys.*, 1989, **90**, 2148; S. Li, H. S. White and M. D. Ward, *Chem. Mater.*, 1992, **4**, 1082; S. Z. Goldberg, R. Eisenberg, J. S. Miller and A. J. Epstein, *J. Am. Chem. Soc.*, 1976, **98**, 5173; P. J. Kunkeler, P. J. van Koningsbruggen, J. P. Cornelissen, A. N. van der Horst, A. M. van der Kraan, A. L. Spek, J. G. Hasnoot and J. Reedijk, *J. Am. Chem. Soc.*, 1996, **118**, 2190.
32 P. Lacroix, O. Kahn, A. Gleizes, L. Valade and P. Cassoux, *New J. Chem.*, 1984, **11**, 643.